Biomimetic Surfaces with Hierarchical Structure using Microsized Texture and Nanosized Cu Particles for Superhydrophobicity

Liguo Qin[1, *2], Hao Yang[1, 2], Xinan Feng[1, 2], Mahshid Hafezi[1, 2], Mawignon Fagla Jules[1, 2], Bin Liu[3], Hui Zhang[1, 2], Guangneng Dong[1, 2], Yali Zhang[4*]

[1]*Key Laboratory of Education Ministry for Modern Design & Rotary-Bearing System, Xi'an Jiaotong University, Xianning West Road, Xi'an, 710049*
[2]*Xi'an Jiaotong University, Institute of Design Science and Basic Component, Xianning West Road, Xi'an, 710049*
[3]*Xi'an Jiaotong University, Institute of Robotics & Intelligent Systems, Xianning West Road, Xi'an, 710049*
[4]*Xi'an Jiaotong University, Key Laboratory of Biomedical Information Engineering of Ministry of Education, Xianning West Road, Xi'an, 710049*

*Corresponding author: E-mail: liguoqin@xjtu.edu.cn, yalee@163.com; Tel: (+86) 18629691717

Received: 05 December 2018, Revised: 21 January 2019 and Accepted: 22 February 2019

DOI: 10.5185/amlett.2019.2252
www.vbripress.com/aml

Abstract

Currently there is a huge demand for the application of superhydrophobic surface in industrial and marine equipment. In this investigation, the hydrophobicity of Q235 steel surface was achieved by implementing micro-patterns on substrate using laser surface texturing and deposition of nano copper particles. By controlling the movement of the laser spots, different controlled textures at micro scale were fabricated. Via the chelation between the copper species and the catechol moieties on polydopamine (PDA), nano copper was decorated to form the multi-level structure. The surface microstructure, topographies, chemical component and wettability of as-prepared superhydrophobic surface were analyzed systematically. Based on the models built by Wenzel and Cassie–Baxter, the effect of micro texture on contact angle was discussed. This method is expected to have many potential applications including antibacterial materials for the protection of marine equipment. Copyright © VBRI Press.

Keywords: Laser ablation, Lotus structure, PDA, nano copper, superhydrophobic.

Introduction

Biomimetic surfaces mean mimicking biology or nature, which allows biologically inspired design, adaptation, or derivation from nature. Biomimetics-inspired materials and surfaces are eco-friendly or green which have generated significant interest and are beneficial in shape green science and technology. Amongst, superhydrophobic surfaces (lotus surface) with a water contact angle (CA) higher than 150° have been attracted great interests due to their importance in both fundamental research and practical application, such as template replication for polymers [**1, 2**], low-drag surfaces for microchannels [**3**], anticorrosion and self-cleaning fabric [**2**]. In order to achieve high contact angle, various surface modification techniques were developed. Among different techniques, using laser irradiation to modify the surface topography at the micro scales is considered as an excellent option [**4**]. By controlling the path of laser irradiation, complex structure or micro patterns can be fabricated on various materials. This technique, being without mask, controllable, and flexible, can introduce various kinds of micro/nanostructures on almost any kind of metal, including iron [**3, 5**], copper [**6**], aluminum [**7**], titanium [**8**], and their alloys. Most of these studies normally focus on the fabrication of different kinds of surface microstructures for hydrophobicity. Because the height and interval of surface micrometer-scale structures can be regulated over wide ranges, this technique provides a perfect tool for studying the influence of various surface microstructures on the surface wettability.

On the other hand, strategies for fabricating superhydrophobic surfaces are of great interest due to their potential applications in metal biofouling prevention and drag reduction in fluid flow [**9**]. Superhydrophobic surfaces were inspired from nature, such as the lotus and rose [**10**]. The superhydrophobic behavior of this leaf, known as the lotus effect or self-cleaning effect, has been found to derive from the micro/nano hierarchical structure and the wax layer present on the leaf surface. Therefore, the hierarchical structure of inorganic particles with super hydrophobicity has become an interesting topic in materials science. Copper nano particles, one of the heavy metals, have been demonstrated for their effectiveness in anti-bacteria performance [**11**]. To generate superhydrophobic surfaces with a hierarchical structure, laser surface textures and copper particles were used as a roughness enhancement material at micro and nano scale, respectively.

Therefore, the objective of this research is to introduce a hierarchical structure on Q235 steel and achieve the performance both in superhydrophobic and self-clean for marine equipment application. The proposed procedure is described in detail in (**Fig. 1**. Firstly, laser surface texturing was carried out with a grid pattern. Then, polydopamine (PDA) that was able to be adhered on virtually all types of material surfaces was used to introduce the interlayer on the substrates. Subsequently, copper was reduced and plated on PDA probably via the chelation between the copper species and the catechol moieties on PDA. The influence of surface micro/nanostructures on the wettability stability was systematically investigated. The microstructure, composite and the Cassie-state stability wettability were systematically investigated.

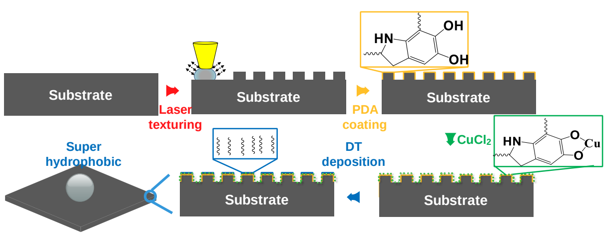

Fig. 1. Illustration of the proposed substrate-independent strategy to fabricate superhydrophobic surfaces based on the sequential modification of laser texturing, PDA, copper and 1-dodecanethiol (DT).

Experimental

Commercial Q235 steel disks (diameter = 30 mm, height = 5 mm) were employed as the substrate materials. The 1-dodecanethiol (DT) was used as the low-surface-energy modifying agent. All chemical reagents in this experiment were used directly without any additional process. Prior to laser texturing process, the Q235 steel surface was polished continuously by #400, #800 and #1600 sandpaper to obtain a smooth surface and the Ra roughness of achieved surface was 0.080 ± 0.012 μm. Then the polished steel was ultrasonically cleaned in ethanol and rinsed thrice by distilled water. Finally, the samples were dried for further process. Laser surface texturing was carried out with a grid pattern (**Fig. 2**), which showed isotropic superhydrophobic properties in all directions with trapped air [**12**]. Three different step sizes (P = 100, 150, and 200 μm) were studied. The grid (L) was kept constant to 50 μm. A compact nanosecond laser fiber machine (QC-F20) with wavelength of 1064 nm was used. During the fabricating process, the focused laser beam was delivered by a galvanometer scanner and F-Theta focusing lens, and the laser pulse duration and peak fluency were 200 ns and 20 J/cm^2 respectively. The average output power, laser repetition frequency and scanning speed were fixed at 20 W, 20 kHz and 600 mm/s, respectively. After the laser manufacturing process, the substrates were ultrasonically cleaned in ethanol and then rinsed with distilled water. Finally, the cleaned steel plates were dried thoroughly in an electrical oven for the following surface process and characterization.

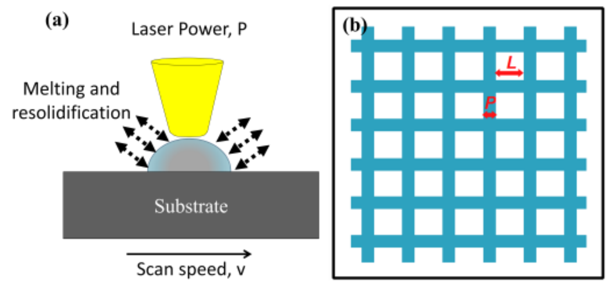

Fig. 2. Schematic illustration of the fabrication of micro rough structure.

The sequential deposition of PDA, Cu and DT was performed by immersing the substrates into different solutions at room temperature (24 ± 2 ºC). The composition of these solutions and the allowed reaction times were as follows:

(1) PDA deposition: 0.1 g dopamine in 50 mL tris(hydroxymethyl) aminomethane (10 mM) HCl buffer solution (pH 8.5), for 3 h
(2) Cu deposition: a mixture solution containing $CuCl_2$ (50 mM), EDTA (ethylene diamine tetraacetic acid, 50 mM), H_3BO_3 (80 mM), and DMAB (dimethylamine broane, 80 mM) with a pH of 7.2, for 8 h
(3) DT deposition: ethanolic solution of DT (60 mM), for 2 h. Acetic acid (20 mM) was added.

Surface morphology, surface chemistry, and surface wettability were investigated by a 3D measuring laser microscope (OLS4000, OLYMPUS), field emission scanning electron microscopy (SEM, SU-8010, HITACHI), energy dispersive spectrum (EDS, oxford INCA Energy), and with an optical contact angle meter (JC2000D2A), respectively. To investigate the durability of the biomimetic superhydrophobic surface, the treated sample was continuously exposed to the water flow from the laboratory faucet at 1.0 m/s for 2 h and then the contact angle was measured. For all the wettability tests, 5 μL of distilled water was dipped on specimen by a microliter syringe, and each specimen was tested thrice to get the mean-value.

Results and discussion

When the laser spot was irradiated on the surface, the bulk material at the center of the laser irradiated zone would be ablated due to the relatively high laser intensity. **Fig. 3** shows SEM images of the surfaces of laser textured samples with different interval of grids. Owing to the overlapping effect of adjacent texture patterns, cavities could be clearly observed on the boundaries. As a result, all samples showed some burrs around the grids. The range of average burr heights, which were measured 5 times with each sample by confocal microscope, was from 16 to 26 µm as shown in **Fig. 4**. This burr formation is not suitable for conventional products, while it is helpful for improving superhydrophobic properties. The contact angle on a rough surface becomes larger than that on a smooth surface when the surface was in hydrophobic state. In addition, the structure can prevent contact of water on the flat area within the grid pattern, so the wetting state can be partial wetting with a hydrophobic surface. Therefore, a rough surface is necessary for a superhydrophobic surface.

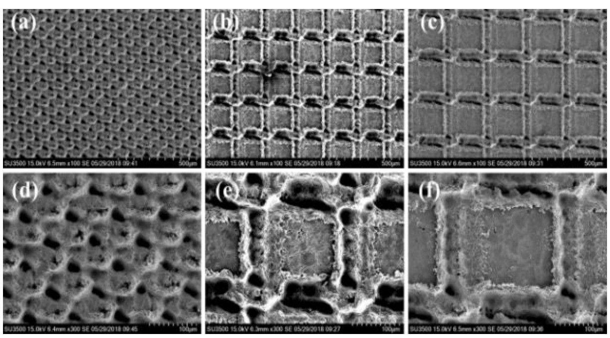

Fig. 3. Irradiated surface images: top images of (a) *P*=100 µm, (b) *P*=150 µm, (c) *P*=200 µm and enlarged tilting image of (d) *P*=100 µm, (e) *P*=150 µm, (f) *P*= 200 µm.

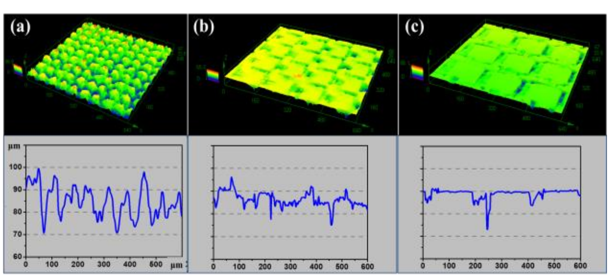

Fig. 4. Confocal microscope images of laser textured samples: (a) *P*=100 µm, (b) *P*=150 µm and (c) *P*=200 µm.

As show in (**Fig. 5**), it can be observed that the polished surface was very clean. After PDA was coated, compact and thin layer was detected. When the substrate was immersed into $CuCl_2$ solution, the following reaction process was happened:

$$2(CH_3)_2NHBH_3+6H_2O+3Cu^{2+}\rightarrow 2(CH_3)_2NH+ 2H_3BO_3+ 6H^+ + 3Cu + 3H_2$$

Cu^{2+} was reduced to Cu (0) by DMAB. The so-reduced copper nanoparticles could be chelated by the catechol moieties on PDA. The diameter of Cu nanoparticles was in the range from 400 nm to 900 nm. Cu and S were found in the EDS spectrum of DT (**Fig. 5d**). **Table 1** summarized the carbon, oxygen, iron and copper content for different samples. Q235-PDA exhibited the highest content of carbon. Q235-PDA-Cu showed the highest content of copper while Q235 was mainly dominated in iron. These confirmed the successive process which was mentioned above.

Table 1. chemical composite of different treated samples.

Sample	C	O	Fe	Cu
Q235	0.12%	0.18%	98.52%	0%
Q235-PDA	18.96%	20.52%	55.36%	0%
Q235-PDA-Cu	8.98%	10.11%	48.19%	16.04%

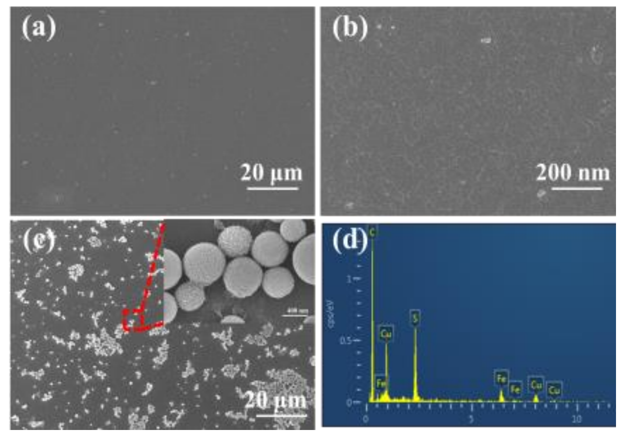

Fig. 5. SEM images of laser textured samples: (a) polished samples, (b) PDA coated surface, (c) copper nanoparticles deposited surface and (d) EDS spectrum of DT coated surface.

The structure and composition of the micro texture and nano copper particle composites were analyzed. EDS-element mapping was obtained and shown in (**Fig. 6**). There typical elements including C, Fe and Cu (**Fig. 6a–c**) were observed. The EDS mapping results indicated that the nano copper particles were successfully deposited after the laser surface texturing. The surface was constructed by bulge (like lotus) at micro and nano scale, respectively.

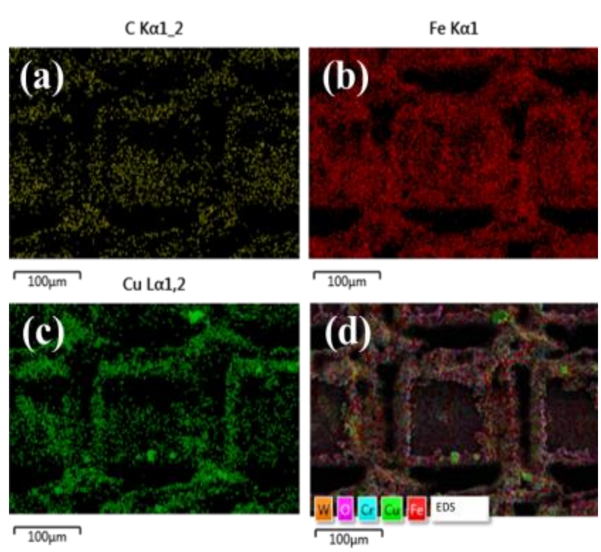

Fig. 6. Element mapping of textured Q235 after further deposition of nano copper particles. (a–d) exhibit the element sensitive maps of C, Fe, Cu and all of them

Controlling wettability of solid surface is crucial for surface engineering, and there are two key factors, surface chemistry and roughness. The wettability of bare Q235, laser textured Q235, PDA modified textured steel, Q235-PDA-Cu and Q235-PDA-DT was illustrated in (**Fig. 7)**. The water contact angle value of bare steel was 38.4°, demonstrating that the carbon steel was in the range of the hydrophilic materials. When the surface texture was created on steel surface, its hydrophilic property was improved with water contact angle value decreased to 23.9°. In fact, such decrease of water contact angle value conformed to the Wenzel model, which described the effect of creating rough structure on the wettability of hydrophobic or hydrophilic materials [**13**]. When PDA was deposited on the substrate, the hydrophilic property was further improved due to the high surface energy. As shown in (**Fig. 7c-e)**, the lowest contact angle was 5°, nearly super hydrophilic.

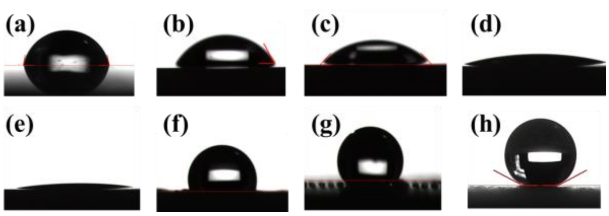

Fig. 7. Photographs of the water droplets on the (a) polished sample, (b) textured surface, (c) PDA modified surface, (d) PDA and textured surface, (e) PDA and textured surface with copper particles, (f) DT modified surface with copper particles, (g) DT modified surface with texture and (h) DT modified surface with texture and copper particles.

After being modified by DT agents, as shown in (**Fig. 7f-g)**, surfaces with texture and copper particles became superhydrophobic with contact angle value increased dramatically to 155.9°, indicating the necessity of the combination of creating multimodal rough surface structure and low-surface-energy coating in fabricating superhydrophobic surface. For fabricating effectively water repelling surface, trapped air in its rough structure and formed an effective air film between the steel surface and water droplet were the fundamental mechanism. The wetting mode of as-prepared superhydrophilic surface turned to the Cassie-Baxter wetting mode, which was mainly used to describe the heterogeneous wetting regime.

Directly after the laser treatment, an increased amount of carbon was detected on the surface, which was believed to derive from the fast decomposition reaction at the time when the laser beam firstly hit the surface. The high energy from the very short laser pulse activated the decomposition reaction and resulted in the initial carbon deposition on the irradiated surface. However, the carbon from this initial fast decomposition is not enough to cover the entire structure. This intrinsic hydrophilicity of the polar iron oxides was then enhanced by the surface roughness according to Wenzel's theory.

As shown in (**Fig. 8)**, the value of contact angle was recorded every half hour. At 0 h, the surface with grid distance of 100 um showed the highest contact angle. In the case of texture and nano copper modified surface, this can be explained by Cassie–Baxter equation [**14**]:

$$\cos\theta w=\Phi s(\cos\theta e+1)-1$$

Here Φs is the area ratio between solid–liquid contact. It reflects the relationship between apparent contact angle (θw) of the composite interface and its intrinsic contact angle (θe). The surface becomes more hydrophobic with the Φs increasing. The grid patterned burr with a hydrophobic material can support water droplets. The contact between the flat surface and water droplet can be prevented with a partially wetted state. As shown in (**Fig. 4)**, Φs was decreased with the distance of grid increasing. Therefore, the surface with grid distance of 100 um showed the highest contact angle. The contact angles of all investigated surfaces decrease as time prolonged, while the decline the evolution of contact was varied. The magnitude of controlling wettability for three dimple shapes with the same p/d is as follows: bigger Φs has the better controlling of wetting behaviors.

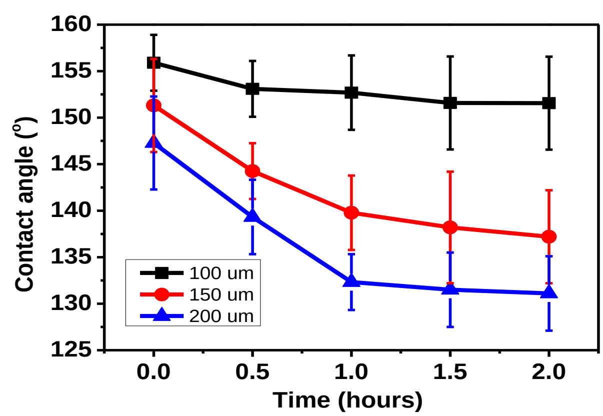

Fig. 8. The evolution of contact angle with wetting surfaces.

On the other hand, considering most of practical applications, superhydrophobic surface must keep stable for a long time, which is very difficult to achieve. The treated sample was continuously exposed to the water flow from the laboratory faucet at 1.0 m/s for 2 h. The evolution of contact angle was shown in (**Fig. 9)**. It can be observed that the surface was quite stable.

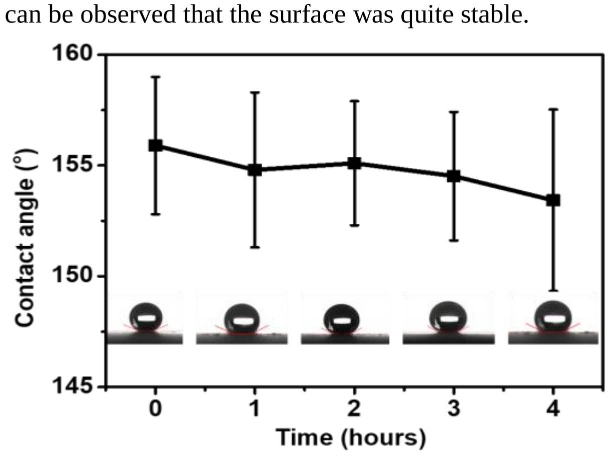

Fig. 9. The evolution of contact angle with water flow.

Usually, the super-hydrophobic property gradually weakens after exposing a few hours under humid conditions. Results showed that the sample surface still maintained almost the same hydrophobicity. That is to say, little damage of the hierarchical structures on the surface was happened and the dual-biomimetic surface can exhibit excellent long-term stability. The reason for it is partly due to the strong bonding of nano-copper particles with the laser textured substrate.

Based on the understanding of the multi-level structures of biological surfaces, the future investigation into bio-inspired multi-functional surfaces can focus on the combination of various biomimetic structures by incorporating multiple technologies of forming various surface topologies so as to fabricate the prepared surface exhibiting excellent comprehensive properties close to the real biological surfaces as far as possible. The artificial surfaces inspired by the lotus leaf have showed unique properties and broad application prospects. Although the relationship between the nano- and micro-scale topographies and the surface properties has not been fully understood, it can be predicted that a biomimetic multi-functional surface bearing the characteristics of both self-cleaning and anti-biofouling may be produced.

Conclusions

In this paper, a method of fabricating micro and nano topologies was demonstrated to fabricate the super-hydrophobic surface. The micro textured surface is based on the melt and solidification of substrate under the control of laser scanning. Nano copper particles possess a great flexibility in manufacturing the surface with nano structure. The hierarchical roughness structures were fabricated and a contact angle model was appointed. The maxim CA of the fabricated super-hydrophobic surface is as high as 157° with the grid size of 0.1 mm. Using the flow washing method, the surface can maintain super-hydrophobic performance as long as possible. This biomimetic surfaces are beneficial in developing nanomaterials, micro/nano devices, and processes with excellent performance in self-cleaning, low adhesion, and drag reduction. Furthermore, it is believed that this method can offer an effective strategy and promising industrial applications for fabricating superhydrophobic surface on other metallic materials.

Acknowledgements

This work was supported by “the Fundamental Research Funds for the Central Universities”. The authors acknowledge the joint financial support from the National Natural Science Foundation of China (51605370 and 51475358), Postdoctoral Science Foundation of Shaanxi Province (2017BSHEDZZ122), China Postdoctoral Science Foundation funded project (2016M602802) and the Natural Science Fund of Shaanxi Province (2017JQ5009). We thank Mr Ren at instrument analysis center of Xi'an Jiaotong University for his assistance with SEM analysis.

Author’s contributions

Conceived the plan: Liguo Qin, Guangneng Dong, Yali Zhang; Performed the experiments: Hao Yang, Xinan Feng; Data analysis: Mahshid Hafezi, Mawignon Fagla Jules, Bin Liu, Hui Zhang; Wrote the paper: Liguo Qin. Authors have no competing financial interests.

References

1. Liu, X. J.; Wu, W. C. X. L.; Wang, Luo, Z. Z.; Liang, Y. M.; Zhou, F.; *Soft Matter*, **2009**, *5*, 3097.
2. Chen, S. S.; Li, X.; Li, Y.; Sun, J. Q.; *Acs Nano*, **2015**, *9*, 4070.
3. Cha, T. G.; Yi, J. W.; Moon, M. W.; Lee, K. R.; Kim, H. Y.; *Langmuir*, **2010**, *26*, 8319.
4. Vorobyev, A. Y.; Guo, C. L.; *Laser Photonics Rev.*, **2013**, *7*, 385;
5. Wu, B.; Zhou, M.; Li, J.; Ye, X.; Li, G.; Cai, L.; *Appl. Surf. Sci.* **2009**, *256*, 61.
6. Long, J. Y.; Fan, P. X.; Zhong, M. L.; Zhang, H. J.; Xie, Y. D.; Lin, C.; *Appl. Surf. Sci.* **2014**, *311*, 461.
7. Long, J. Y.; Zhong, M. L.; Zhang, H. J.; Fan, P. X.; *J. Colloid Interface Sci.* **2015**, *441*, 1.
8. Kietzig, A. M.; Hatzikiriakos, S. G.; Englezos, P.; Langmuir **2009**, *25*, 4821.
9. Mahalakshmi, P. V.; Vanithakumari, S. C.; Gopal, J.; Mudali, U. K.; Raj, B.; *Curr. Sci.*, **2011**, *101*, 1328
10. Yao, X.; Song, Y. L.; Jiang, L.; *Adv. Mater.*, **2011**, *23*, 719.
11. Borkow, G.; Gabbay, J.; *Curr. Med. Chem*, **2005**, *12*, 2163.
12. Chun, D. M.; Davaasuren, G.; Ngo, C. V.; Kim, C. S.; Lee, G. Y.; Ahn, S. H.; *Cirp Ann-Manuf Tech.*, **2014**, *63*, 525.
13. Murakami, D.; Jinnai, H.; Takahara, A.; *Langmuir*, **2014**, *30*, 2061.
14. Cassie, A. B. D.; Baxter, S.; *Trans. Faraday Soc.* **1944**, *40*, 0546.